eLIFE
elifesciences.org

Figures and figure supplements

A suppression hierarchy among competing motor programs drives sequential grooming in *Drosophila*

Andrew M Seeds, et al.

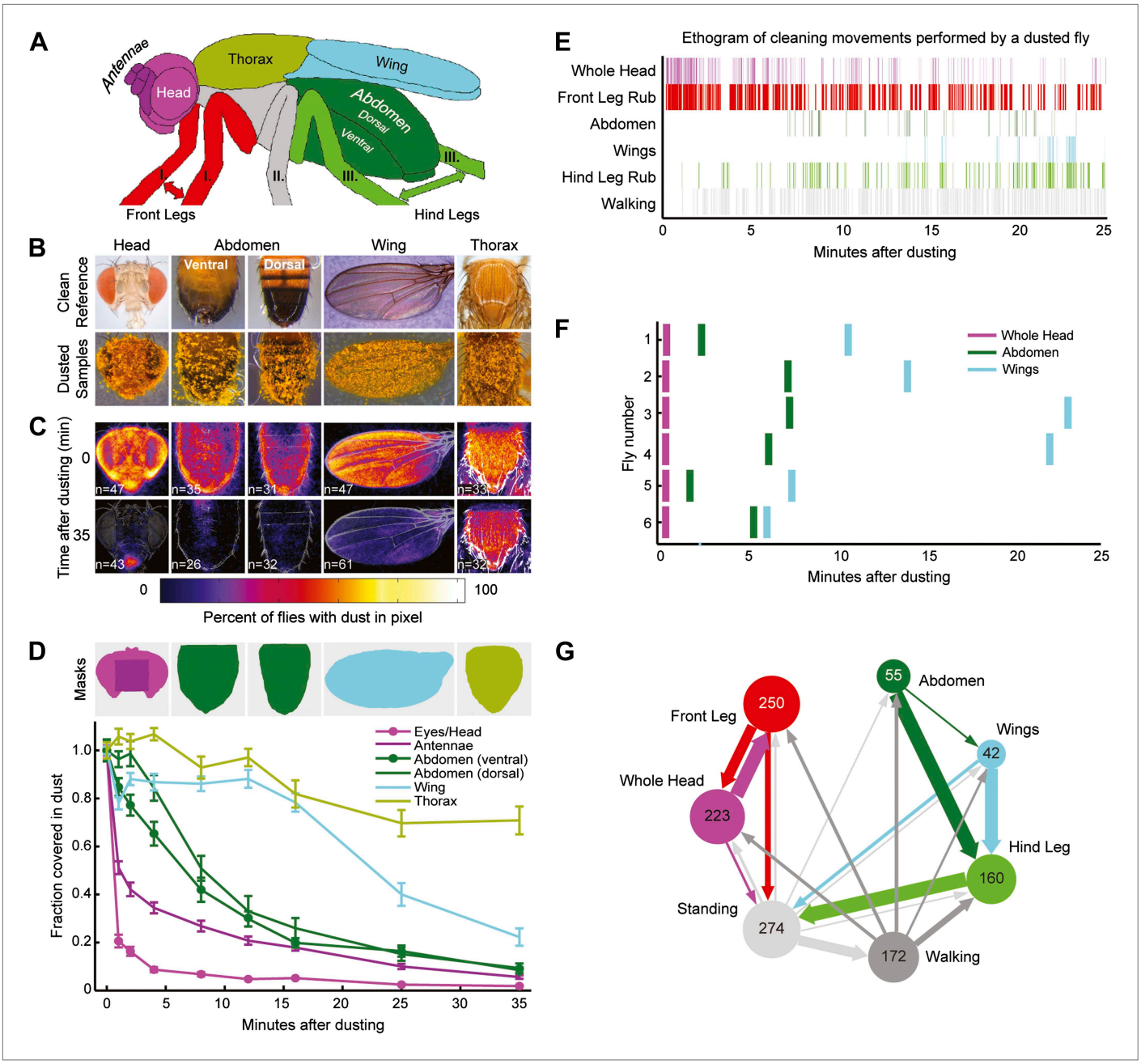

Figure 1. Wild-type flies clean different areas of the body sequentially. (**A**) Diagram of body parts cleaned by front leg (red hues) or hind leg (green hues) movements. (**B**–**D**) Dust distribution measurements of the bodies of flies that were coated in yellow dust and allowed to groom. (**B**) Body parts were imaged (dusted samples) and aligned to clean reference images in order to determine the fraction of dust left on each part. (**C**) Average spatial distribution of dust 0 min after dusting and after flies groomed for 35 min. The number of flies contributing to each heat map is displayed. (**D**) Dust removal across a 35-min time course. Masks define regions for counting the yellow pixels (dust) remaining on each sample. Each time point (normalized to 0-min samples) is plotted as the fraction of dust left in the defined regions and shown as the mean ± SEM; n ≥ 26 flies. Figure panel is compiled from data shown in ***Figure 1—figure supplement 3***. (**E**) Representative ethogram of the five most common cleaning movements performed by an individual fly after dusting (manually scored from video recordings). All head cleaning movements are binned because eye and antennal cleaning are not easily distinguishable in the dusted state using our analysis methods (labeled whole head). (**F**) Latency to the first bout of head, abdomen, or wing cleaning after dusting for each of six flies annotated. (**G**) Transitions among different body cleaning movements, standing, and walking (across a 25-min time course, n = 6 flies). The radii of the nodes are proportional to the log of the average fraction of total cleaning bouts for each movement. Average total bouts for each movement are shown. Arrow widths represent the transition probabilities between the movements (displaying transition probabilities ≥0.05).

DOI: 10.7554/eLife.02951.003

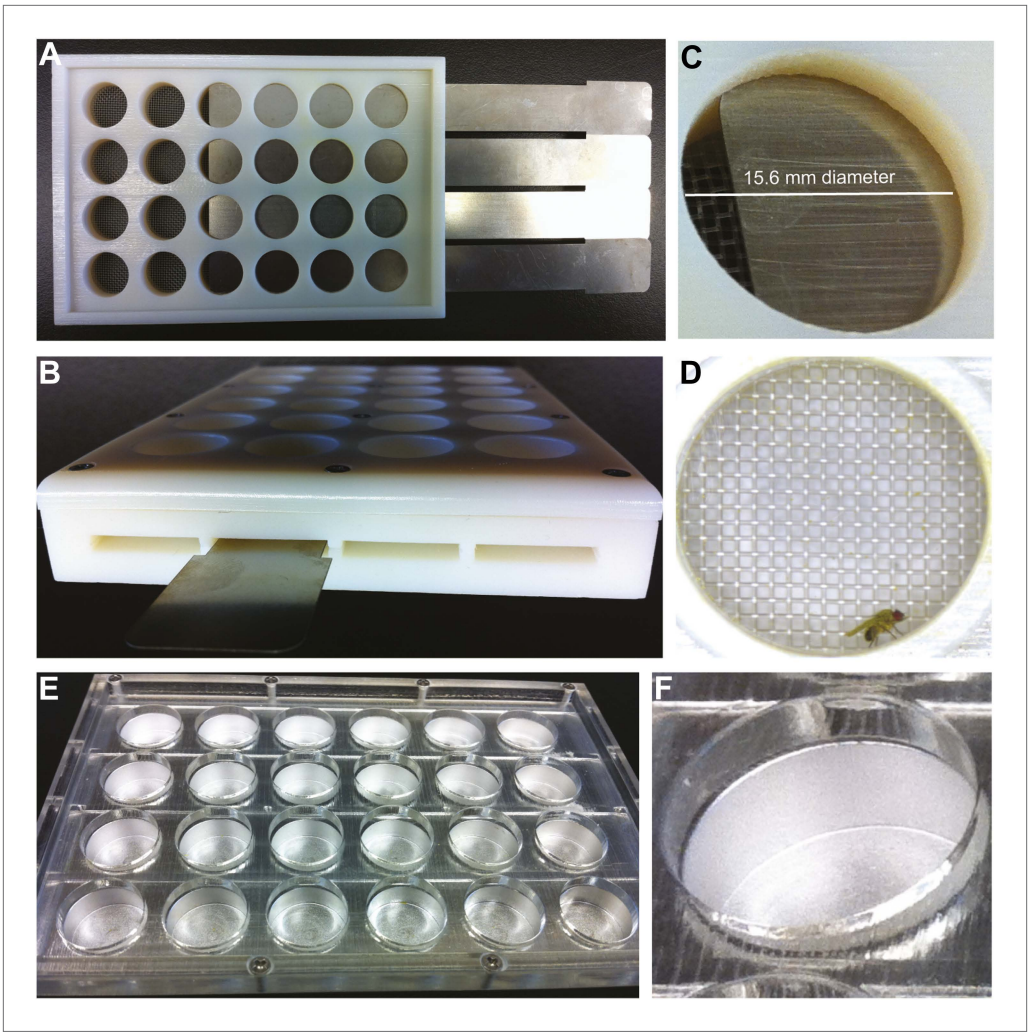

Figure 1—Figure supplement 1. Grooming apparatus for dusting, recording, and observing flies.
DOI: 10.7554/eLife.02951.004

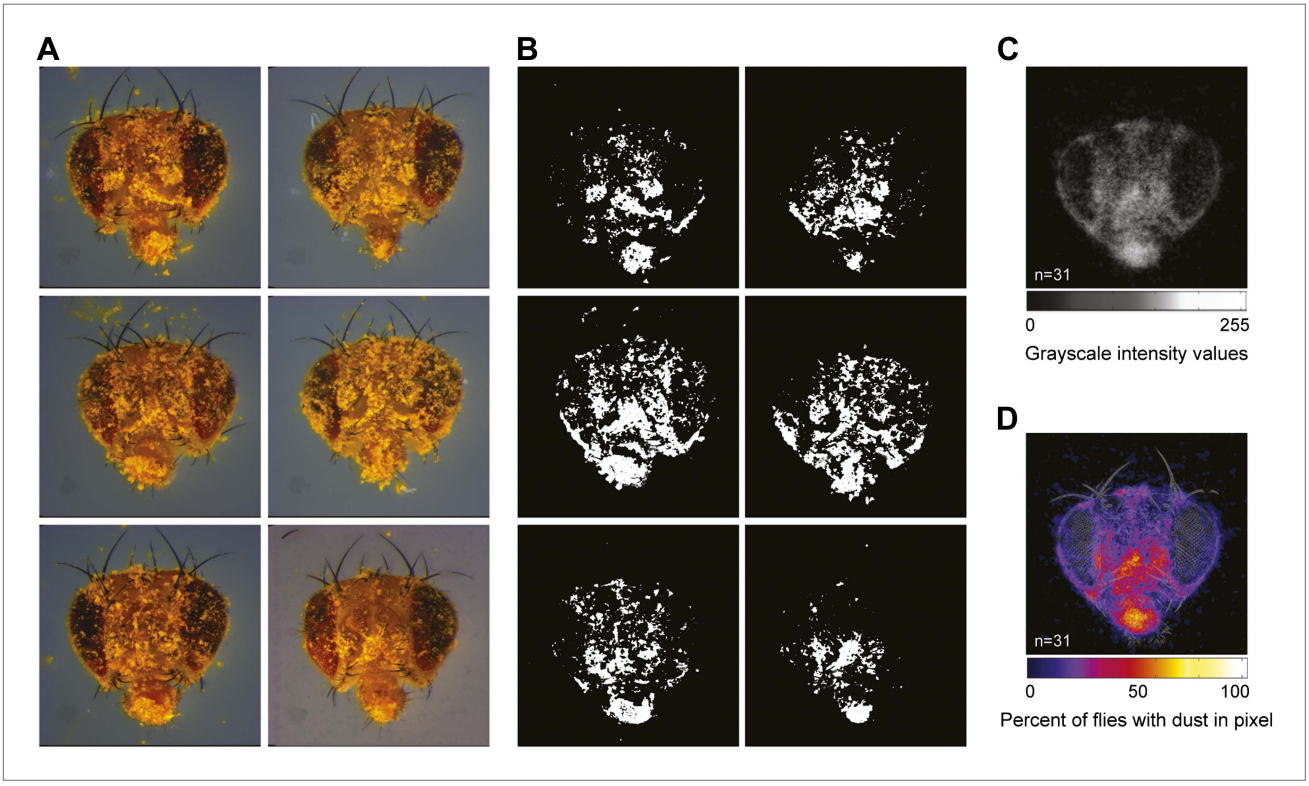

Figure 1—Figure supplement 2. Strategies for quantifying dust on the body surface.
DOI: 10.7554/eLife.02951.005

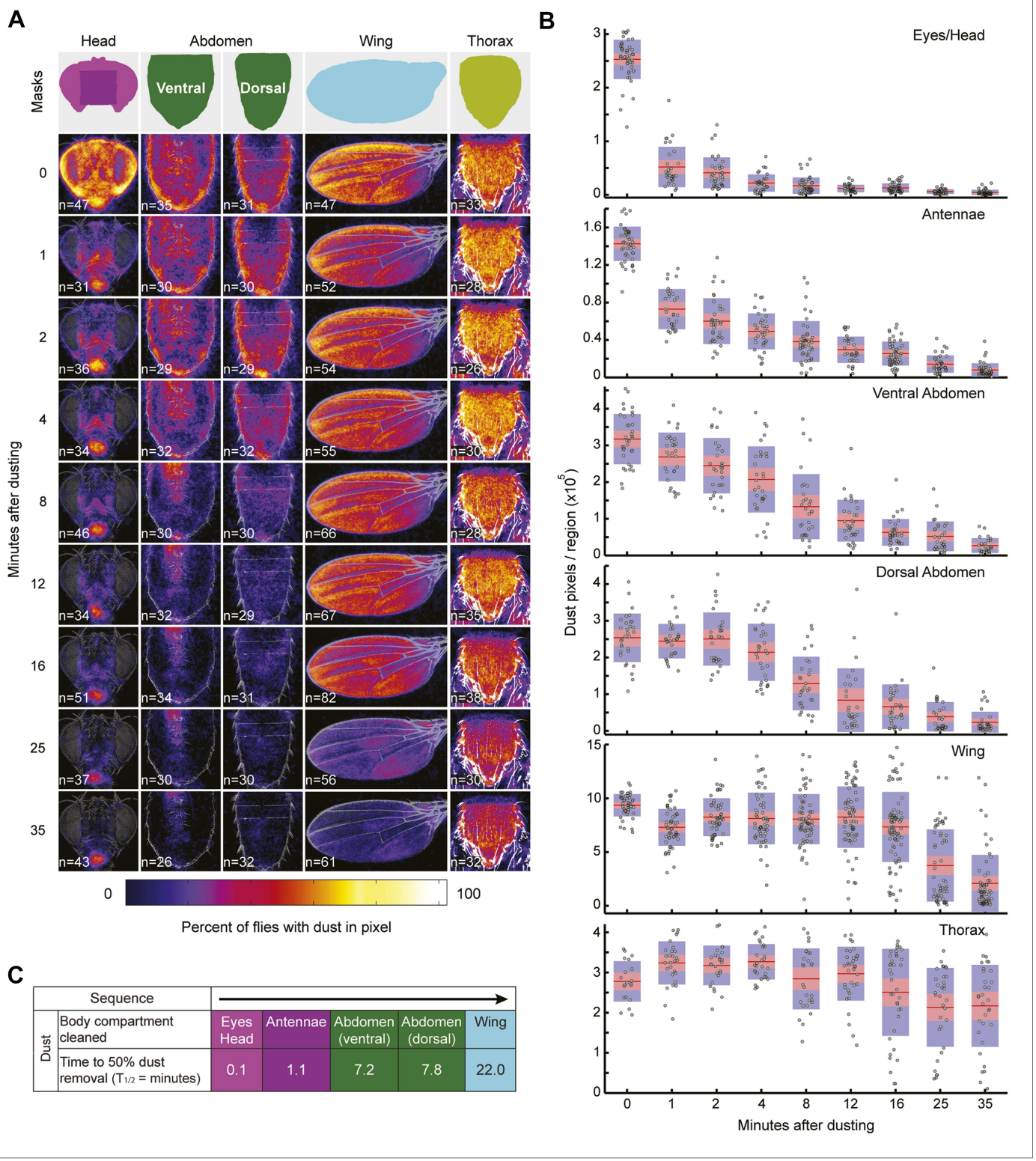

Figure 1—Figure supplement 3. Wild-type flies remove dust from body parts at different rates.
DOI: 10.7554/eLife.02951.006

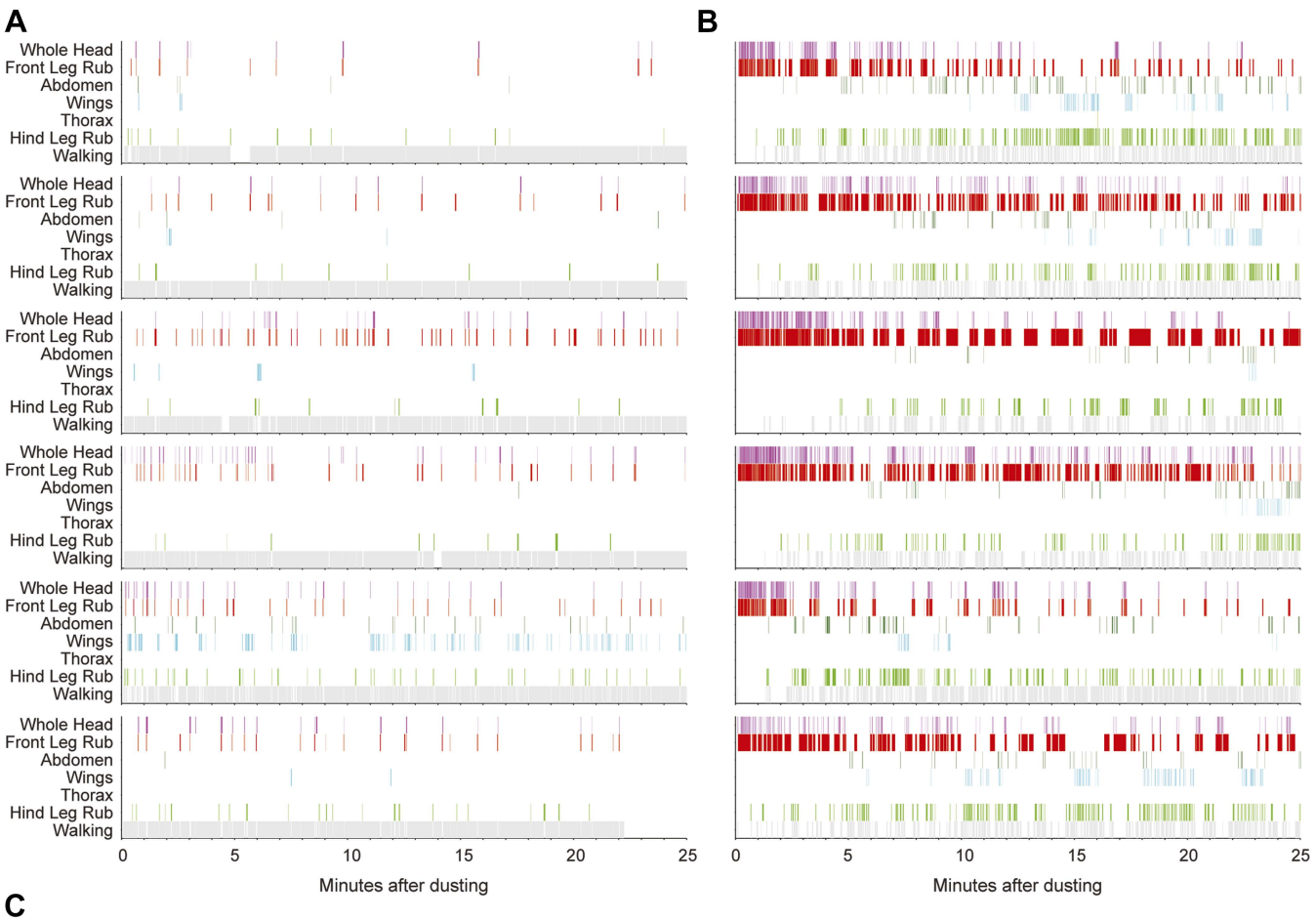

C

	Shaken without dust (mm:ss to first movement)				Shaken with dust (mm:ss to first movement)			
	Head	Abdomen	Wing	Thorax	Head	Abdomen	Wing	Thorax
Fly 1	0:37	0:43	0:45	-	0:10	2:08	10:22	16:01
Fly 2	1:19	0:47	2:01	11.45	0:07	6:59	13:43	-
Fly 3	1:30	-	0:32	-	0:07	7:05	22:43	-
Fly 4	0:09	17:34	-	-	0:07	5:54	21:42	-
Fly 5	0:10	0:35	0:16	-	0:07	1:29	7:12	-
Fly 6	0:43	1:56	7.30	-	0:07	5:03	5:48	-

Figure 1—Figure supplement 4. Sequential cleaning of the head, abdomen, and wings requires dust.
DOI: 10.7554/eLife.02951.007

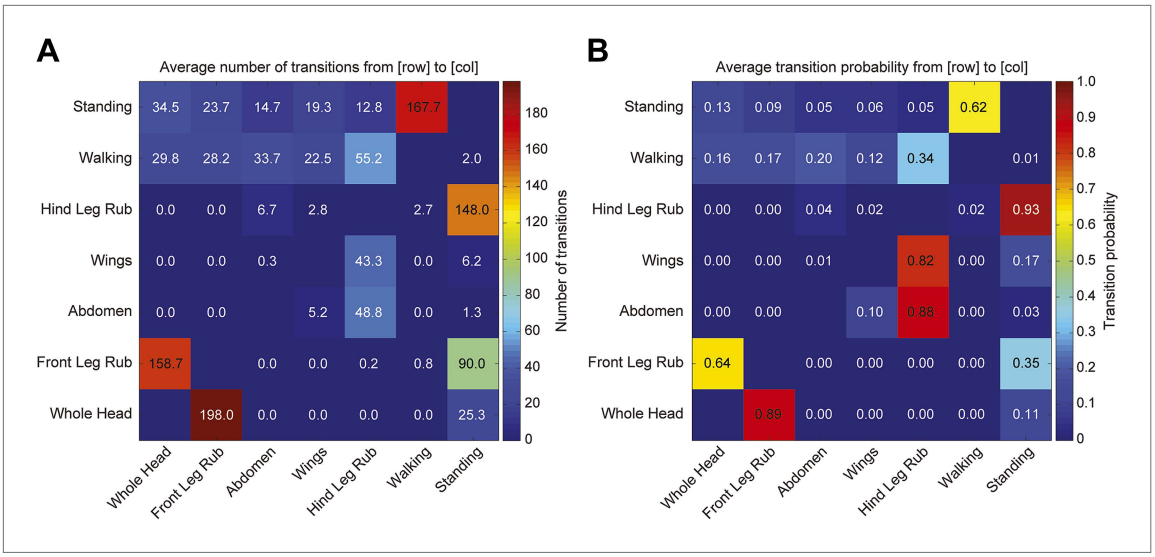

Figure 1—Figure supplement 5. Transitions among cleaning movements of dusted wild-type flies.
DOI: 10.7554/eLife.02951.008

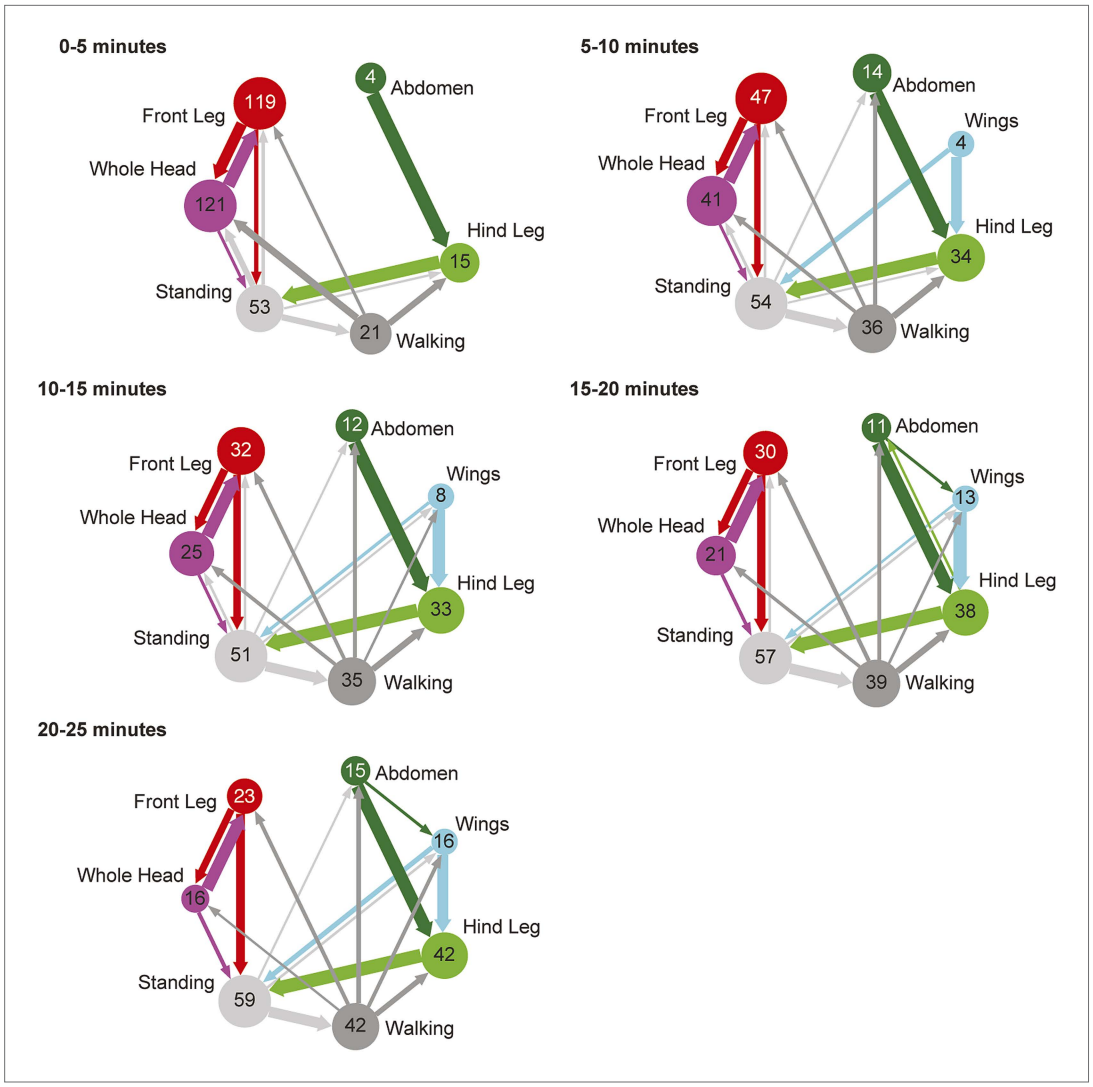

Figure 1—Figure supplement 6. Transitions among cleaning movements performed by dusted wild-type flies over a time course.

DOI: 10.7554/eLife.02951.009

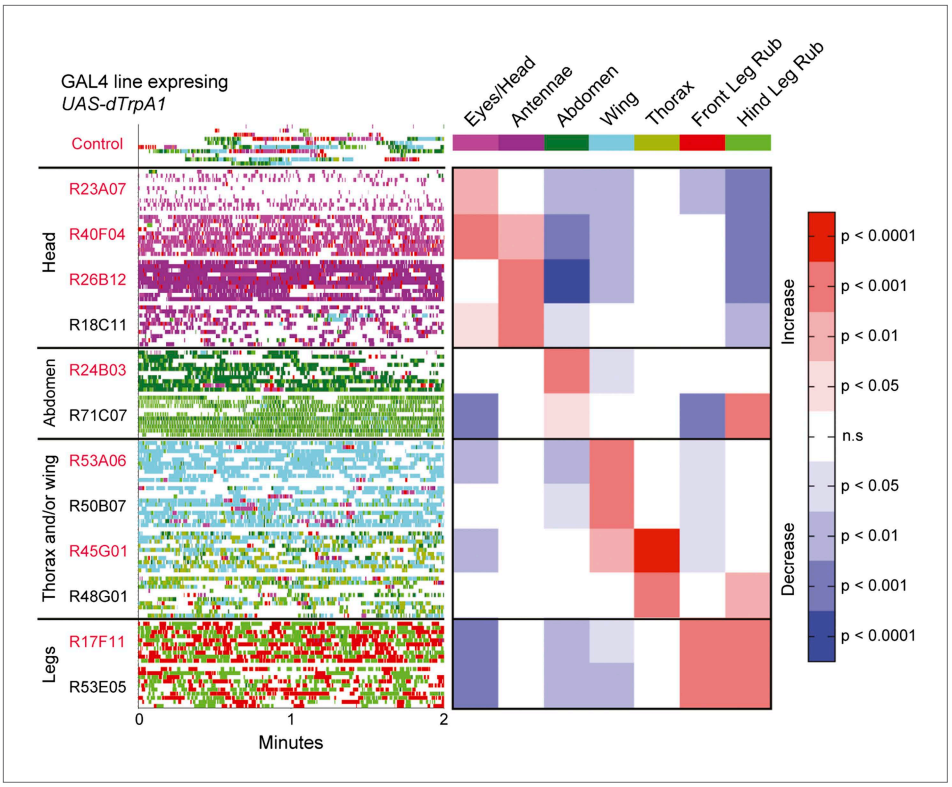

Figure 2. Activation of *UAS-dTrpA1* in different GAL4 lines is sufficient to activate discrete cleaning movements in the absence of dust. Cleaning movement activation phenotypes driven by 12 GAL4 lines expressing *UAS-dTrpA1*. Flies (including controls) were warmed to 30°C to activate the targeted neurons while their cleaning movements were recorded and manually scored (n = 10 flies/GAL4 line; 130 flies total). Ethograms of the scored behaviors are displayed by compressing all mutually exclusive events to a single line per fly. Colors below the movement names correspond to those on the ethograms. White space in each ethogram represents the time flies spent walking or standing in place. The GAL4 lines are grouped into four cleaning movement categories: head, abdomen, thorax and/or wings, and legs. The grid displays increases and decreases from control flies in the fraction of time each line spent performing different cleaning movements. Grid heat map represents the p-values for the comparisons of the different GAL4 lines and control flies (Kruskal–Wallis followed by Mann–Whitney U pairwise tests and Bonferroni correction). Note: R71C07 displays significant increases in both abdominal cleaning and leg rubbing. Although this line is shown in the abdominal cleaning category, it could also be included with leg rubbing. Lines labeled in red are used in experiments shown in ***Figure 3*** and ***Figure 5***. See ***Video 2***, ***Video 3***, ***Video 4***, ***Video 5***, ***Video 6***, ***Video 7***, ***Video 8***, and ***Video 9*** for representative videos and more description of the activation phenotypes of these lines.

DOI: 10.7554/eLife.02951.011

Figure 2—Figure supplement 1. GAL4 lines expressing *UAS-dTrpA1* have different activated cleaning phenotypes at high temperature.

DOI: 10.7554/eLife.02951.012

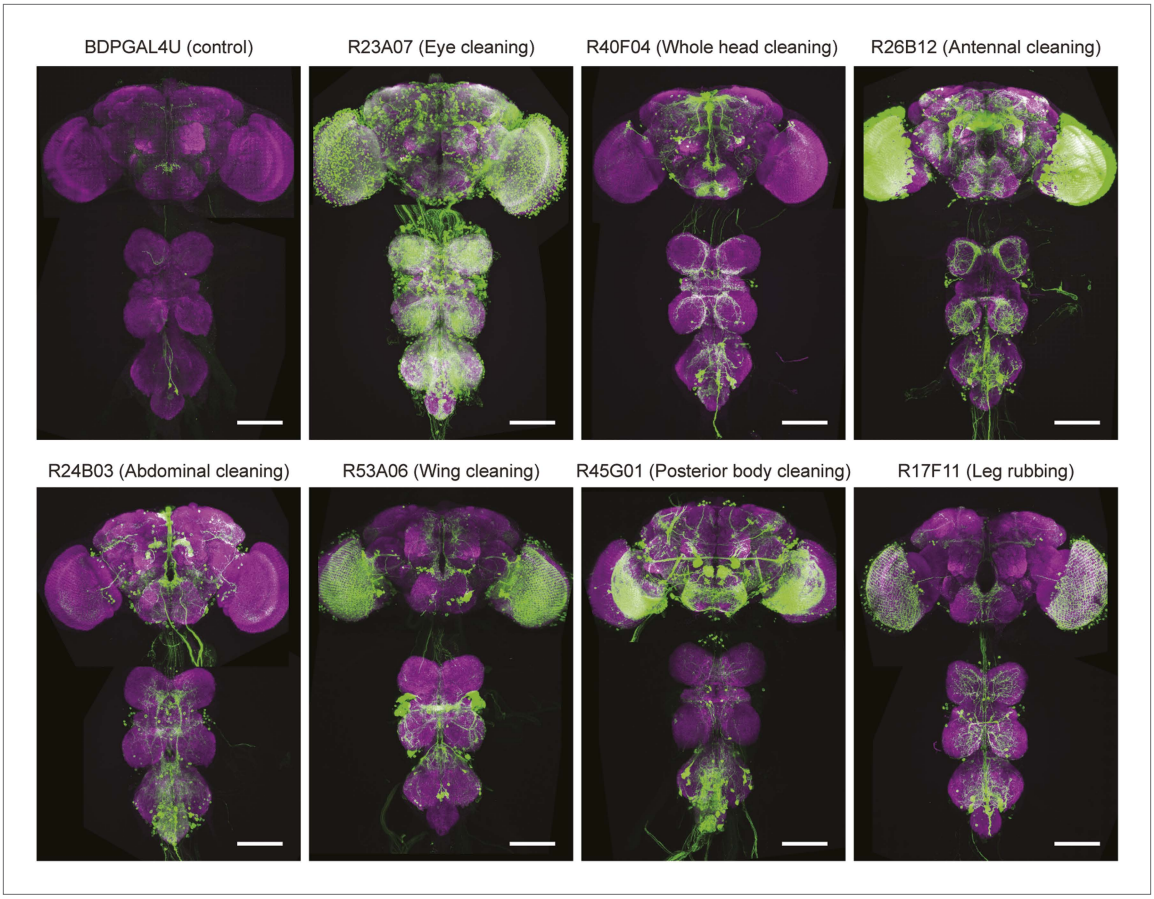

Figure 2—Figure supplement 2. Anatomy of GAL4 lines used to activate distinct cleaning movements.
DOI: 10.7554/eLife.02951.013

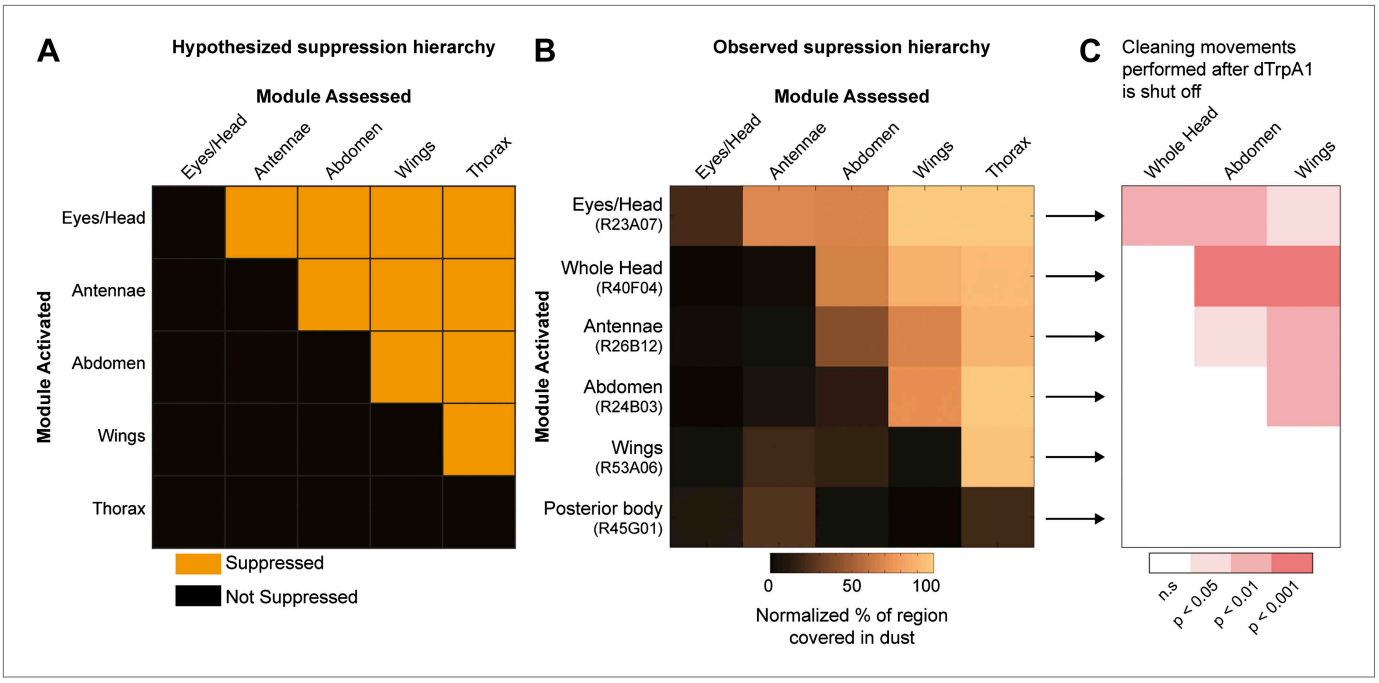

Figure 3. Hierarchical suppression and dust stimulus drive cleaning movement selection. Cleaning of specific body parts was artificially activated while flies were dusted to stimulate competition between their cleaning movements. Flies were pre-warmed at 30°C such that the dTrpA1-induced cleaning module was active at the time of dusting. After grooming for 25 min, flies were anesthetized and their dust patterns were measured. (**A**) Grid showing the expected suppression pattern if the hierarchical suppression hypothesis is true. Modules are arranged on the grid in the order that they occur in the normal grooming sequence. (**B**) The observed suppression hierarchy. For each line, the normalized fraction of dust remaining on different regions of the flies is mapped onto the corresponding grid locations (n ≥ 26 per body part, 'Materials and methods'). The module activated by each GAL4 line is listed above the line name. Data used to generate the grid is shown in ***Figure 3—figure supplement 1***. (**C**) Cleaning movements performed when a GAL4/dTrpA1-activated module is shut off. Arrows from **B** to each row in **C** show the GAL4 line and corresponding dust distribution that was tested. The grid displays increases from control flies in the frequencies of different cleaning movements performed in the first 3 minutes after shutting off dTrpA1 (n = 10 flies per line). Grid heat map represents the p-values for the comparisons of the different GAL4 lines and control flies (Kruskal–Wallis followed by Mann–Whitney U pairwise tests and Bonferroni correction). Movements were manually scored. All head cleaning movements are binned and displayed as whole head, because eye and antennal cleaning are not easily distinguishable in the dusted state. Control and experimental flies performed few thoracic cleaning bouts and are therefore not shown.

DOI: 10.7554/eLife.02951.022

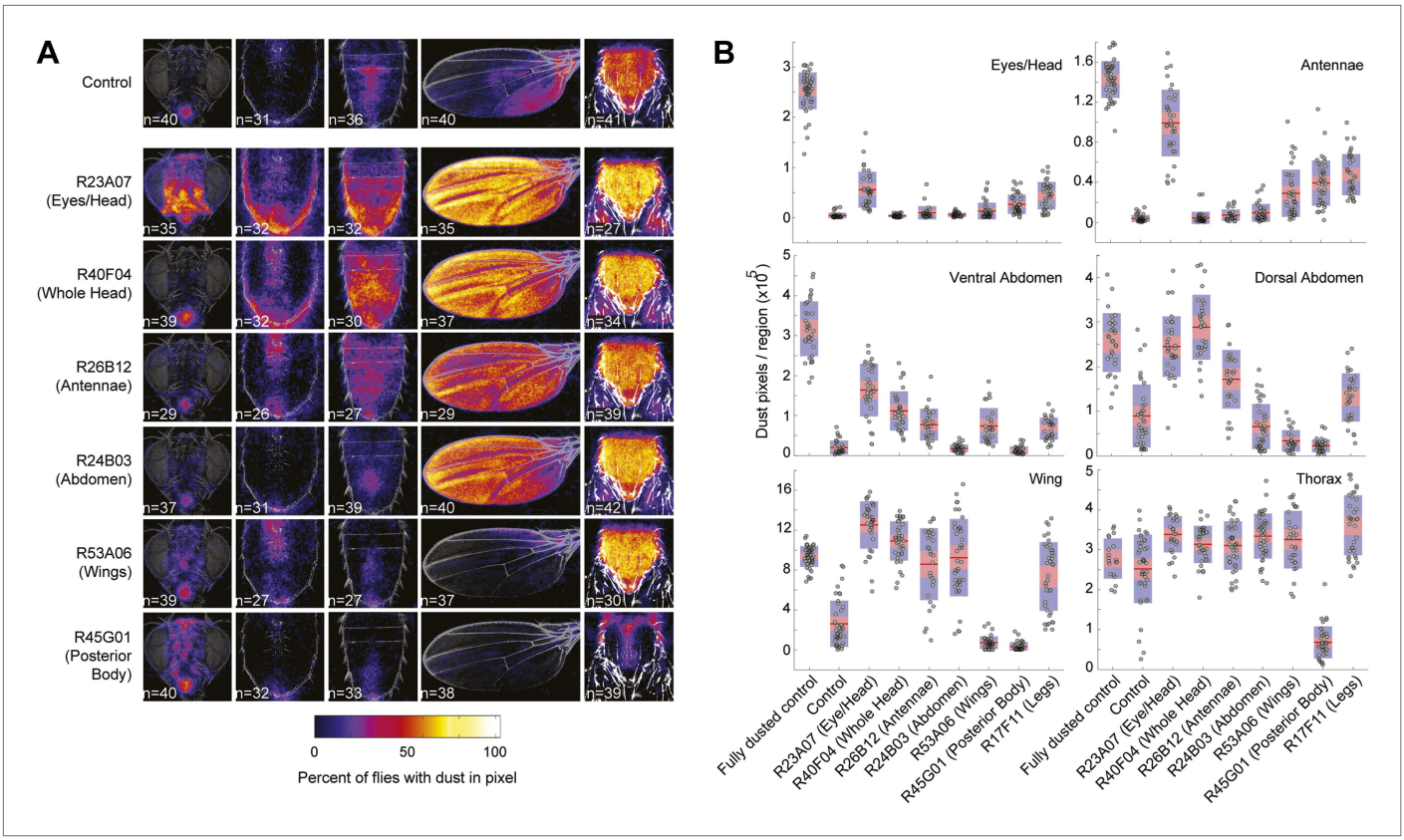

Figure 3—Figure supplement 1. Dust patterns resulting from coating flies in dust and artificially activating specific cleaning movements.

DOI: 10.7554/eLife.02951.023

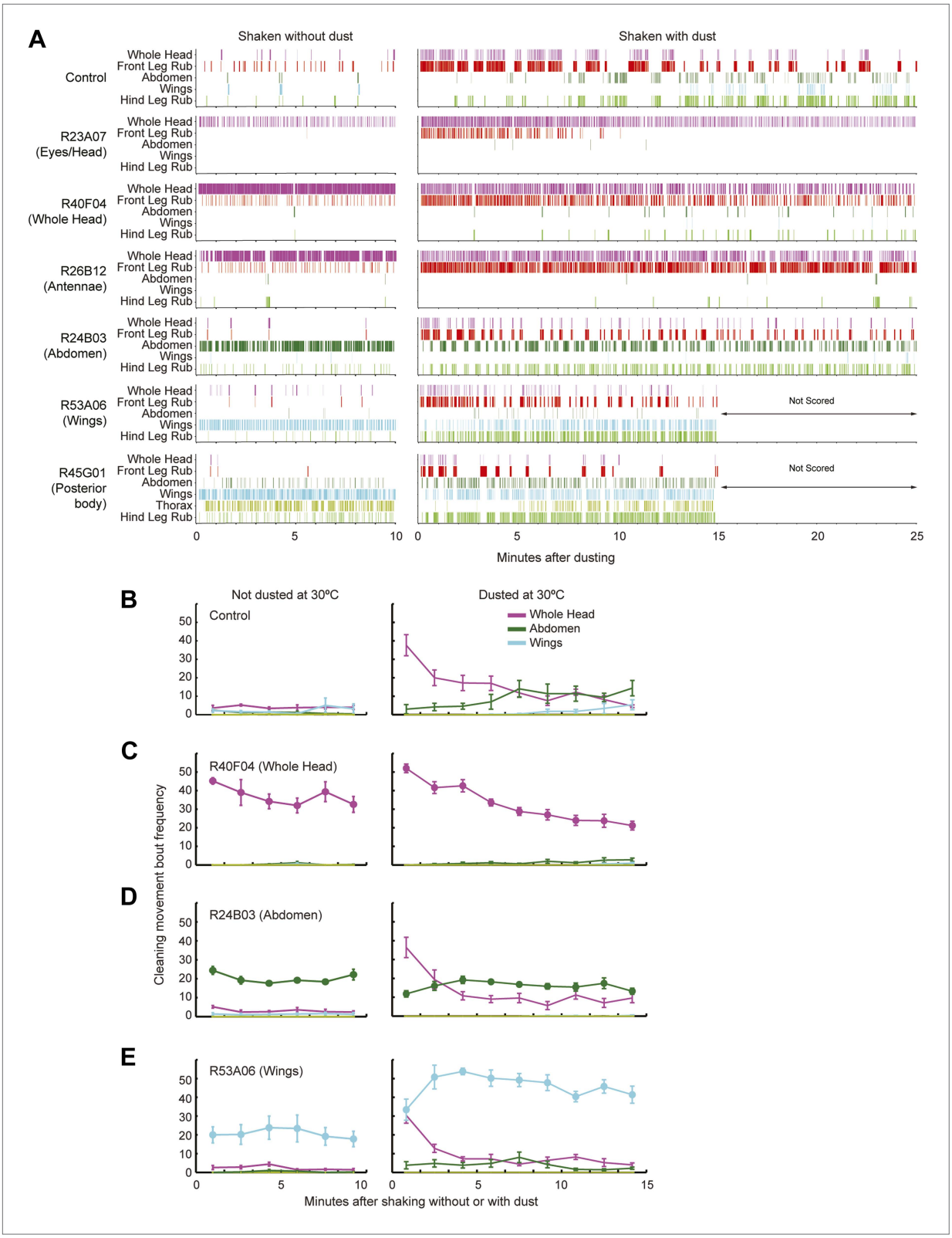

Figure 3—Figure supplement 2. Behaviors of flies that were coated in dust while specific cleaning movements were artificially activated.

DOI: 10.7554/eLife.02951.024

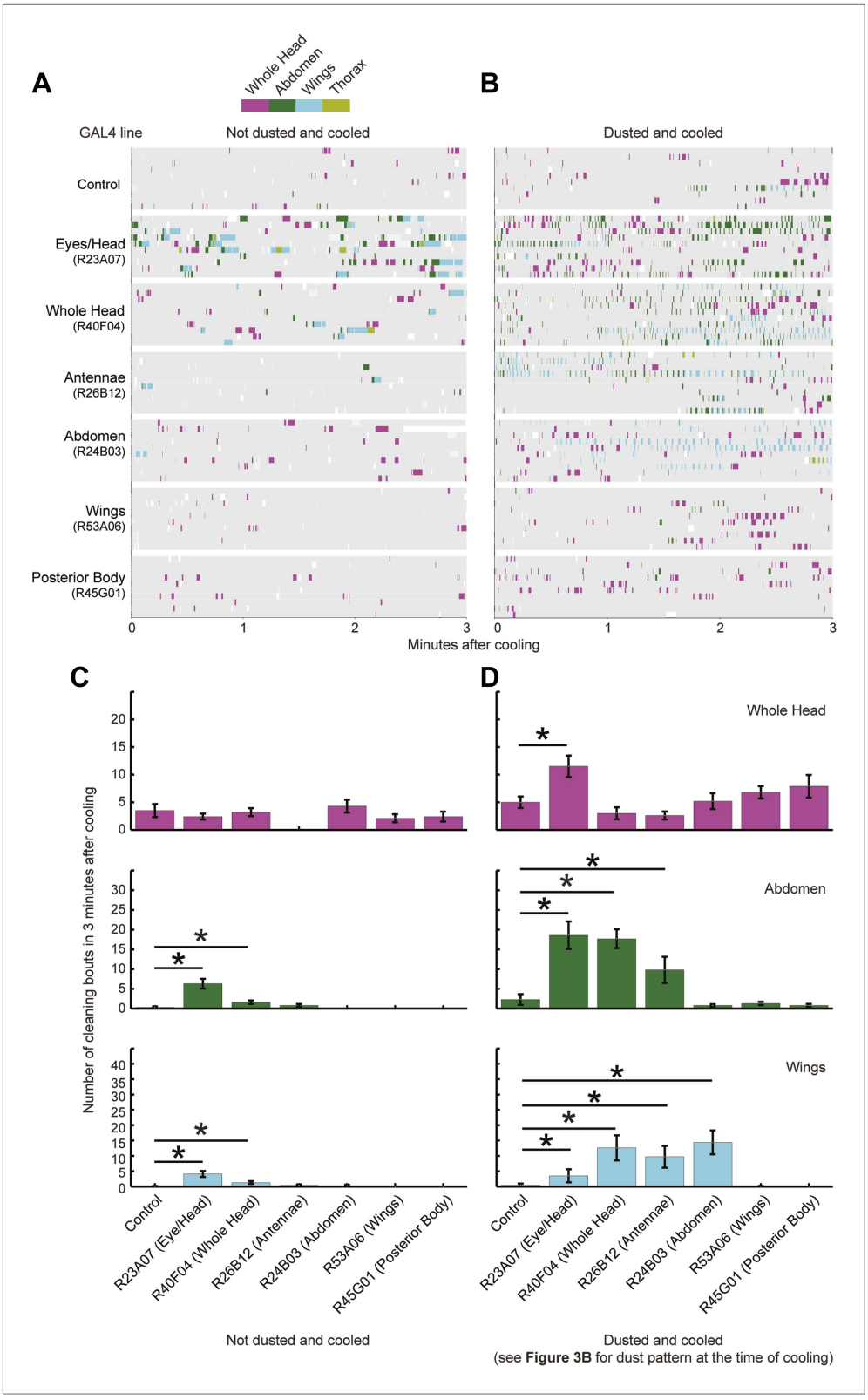

Figure 3—Figure supplement 3. Triggering of cleaning movements is dust dependent.
DOI: 10.7554/eLife.02951.025

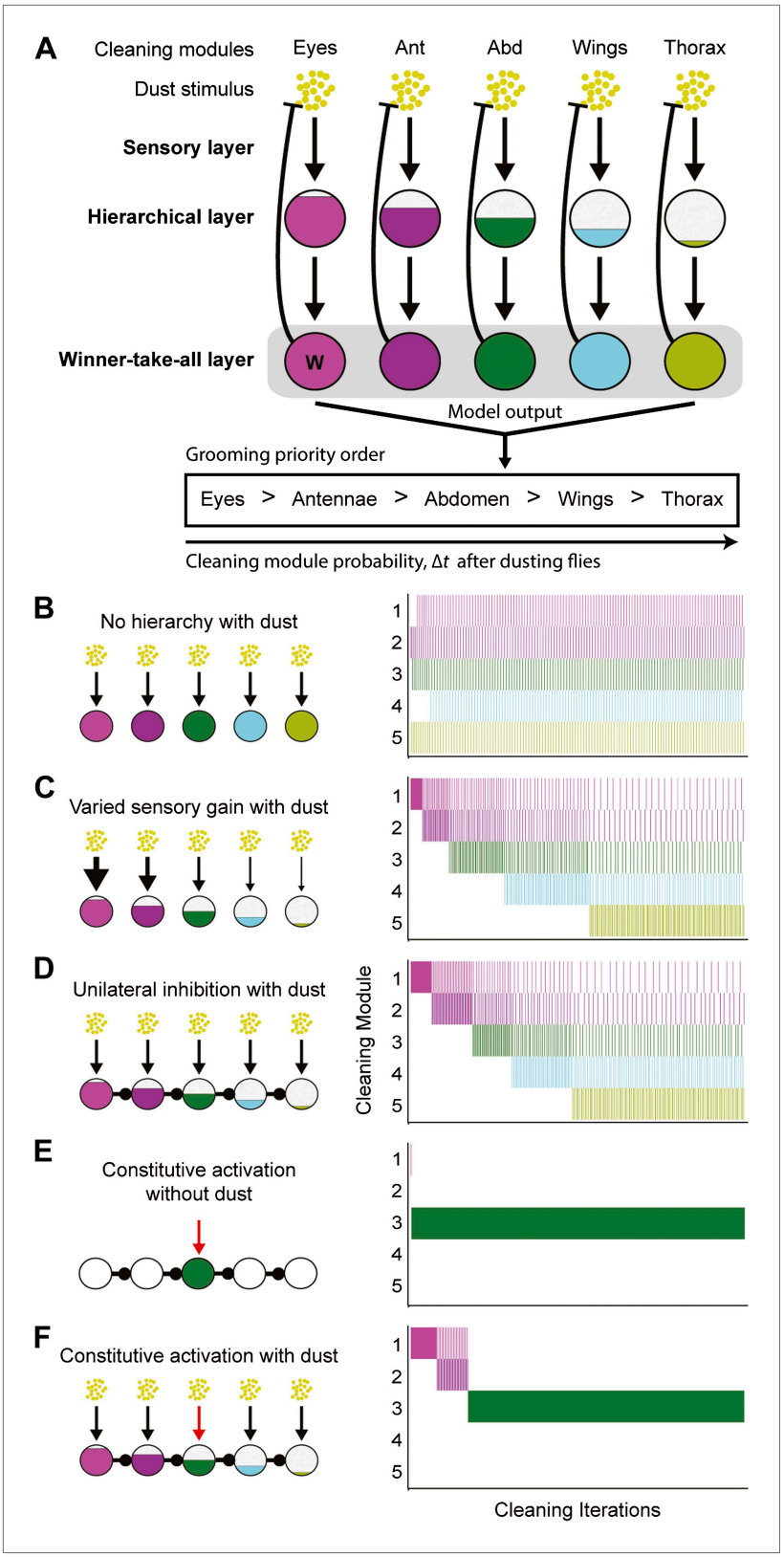

Figure 4. Model of hierarchical suppression results in the sequential progression of grooming. (**A**) The dust induced grooming sequence requires three layers: (1) the sensory layer detects dust and independently activates each cleaning module. This is shown as parallel excitatory arrows from each yellow dust cartoon to activate specific

Figure 4. Continued on next page

Figure 4. Continued

cleaning modules. (2) The hierarchical layer determines each module's level of activation when its respective body part is coated in dust. Circle fill levels show theoretical differences in the relative activation levels of the modules. (3) The winner-take-all layer selects the cleaning module that is most active and suppresses all competing responses ('W' in this layer shows that the eye cleaning module is selected first). Theoretical all-to-all inhibitory connections in this layer are depicted as a gray box for simplicity. Blunt arrows from the winner-take-all layer to the yellow dust depict that the winning module reduces its own sensory input by cleaning off the dust and consequently becoming less active. The cleaning continues until the activation level of the module is no longer maximal, at which point the transition of cleaning to the new maximally active module occurs. Multiple iterations of this process result in a sequential progression. (**B**–**D**) Computational model simulates possible implementations of the hierarchical layer in establishing the most active modules. Modifications to the hierarchical layer and sensory inputs are depicted in each diagram. In this simulation, the competition is between five different cleaning modules. The ethograms show typical results of the simulation, where each row corresponds to the output of a module. (**B**) Equal sensitivities to dust and no inhibitory connections. (**C**) Modules with varying sensory gain in response to dust: modules with higher sensory gain (depicted with thicker arrows) have higher activation levels in response to the same dust amount. Fill levels represent the relative activity levels of the modules at the first iteration of the simulation. (**D**) Unidirectional lateral inhibitory connections between the modules. For simplicity of illustration, only the nearest-neighbor inhibitory connections are shown; in the computational implementation, each module inhibits all the subordinate modules in the hierarchy (e.g., 2 inhibits 3, 4, and 5). (**E**) Constitutive activation of a single cleaning module. Simulated by setting the amount of dust on a particular body part to completely dirty after each round of cleaning (depicted with the red arrow). (**F**) Constitutive activation of a single cleaning module in the presence of dust on all body parts.
DOI: 10.7554/eLife.02951.026

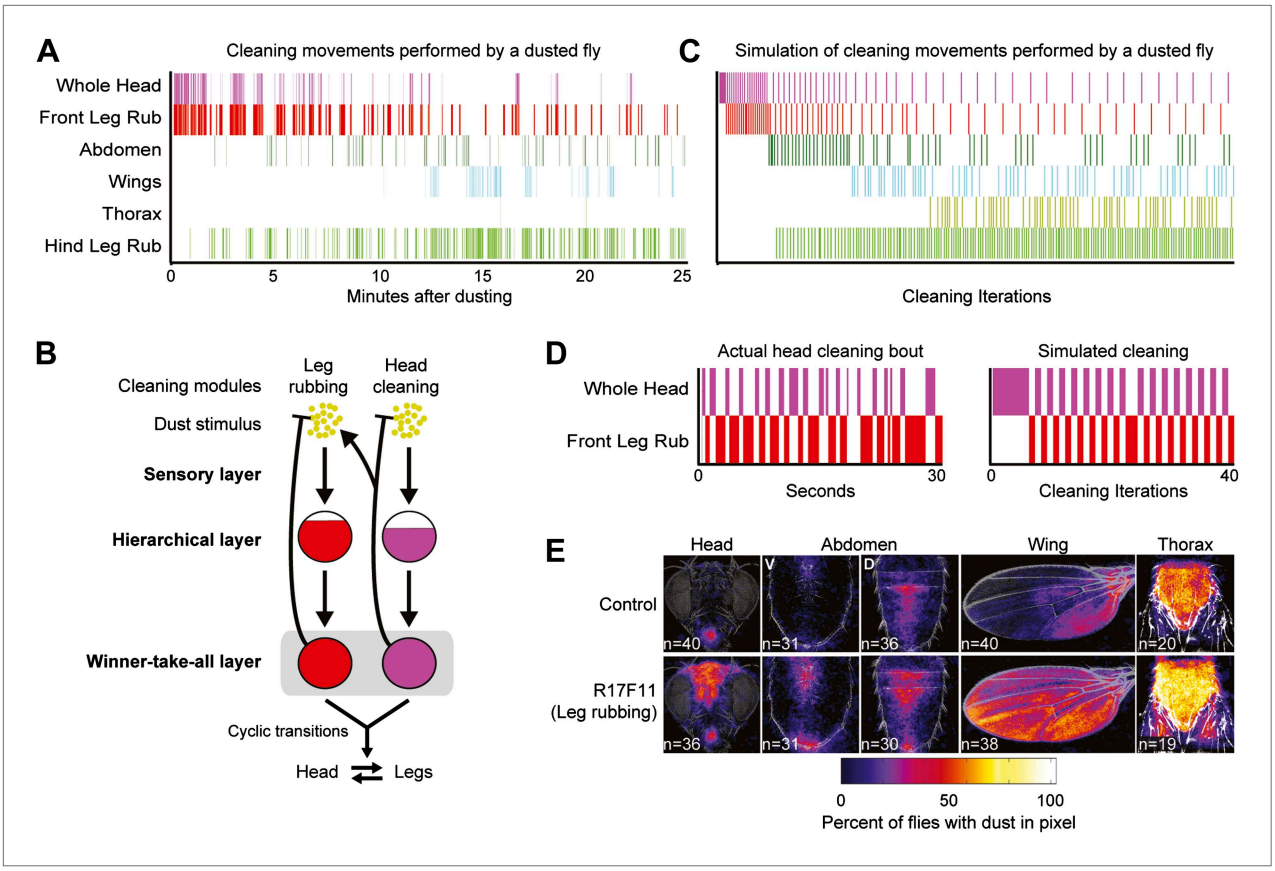

Figure 5. Hierarchical suppression mediates the cyclic transitions between cleaning modules. Leg rubbing was simulated in the grooming model based on two features. (1) The legs accumulate dust as they remove it from the body parts. Leg rubbing is subsequently executed to remove that dust. (2) The sensory gain on the legs was set high relative to the other cleaning modules such that they are the most active and selected in the winner-take-all layer when they were sufficiently dirty. (**A**) Ethogram example of a wild-type fly grooming for comparison to the simulation. (**B**) Model of the leg rubbing and body part cleaning cycle (head cleaning example shown). Leg rubbing is hierarchically associated with the body-cleaning modules (similar to the associations among the cleaning modules described in ***Figure 4***). The only difference between leg rubbing and the other modules is the accumulation of dust on the legs during body part cleaning. This is depicted by a forked connection that removes dust from the head (blunt arrow) and transfers it to the legs (arrow to the leg rubbing module). (**C**) Simulation of grooming with leg rubbing and four body-cleaning modules (result is typical). (**D**) Typical examples of cyclic switching between body cleaning and leg rubbing. The ethogram on the left displays a wild-type fly cleaning its head and the one on the right shows a simulated head-cleaning bout (each example is from early time points in **A** or **C** respectively). (**E**) Average spatial distribution of dust on each body part that remains when flies were coated in dust while leg rubbing was activated (25 min after dusting). V = ventral, D = dorsal.

DOI: 10.7554/eLife.02951.027